ISSN 1063-7842, Technical Physics, 2021, Vol. 66, No. 2, pp. 269–274. © Pleiades Publishing, Ltd., 2021.
Russian Text © The Author(s), 2021, published in Zhurnal Tekhnicheskoi Fiziki, 2021, Vol. 91, No. 2, pp. 281–286.

PHYSICAL SCIENCE OF MATERIALS

# Pseudogap, Nanocrystals and Electrical Conductivity of Doped Silicate Glass

**G. Abdurakhmanov[a,b,*], V. I. Shimanski[c], B. Oksengendler[b], B. Umirzahov[a], and A. N. Urokov[a,**]**

[a] *Tashkent State Technical University, Tashkent, 100095 Uzbekistan*
[b] *National University of Uzbekistan, Tashkent, 100174 Uzbekistan*
[c] *Belarusian State University, Minsk, 220300 Belarus*
**e-mail: gulmirzo@mail.ru*
***e-mail: fyashjon@gmail.com*

Received May 12, 2020; revised August 8, 2020; accepted September 1, 2020

**Abstract**—The ideas of pseudogap and nanocrystals have applied to mechanism of electrical conduction in silicate glass doped by oxides of transition metals (thick film resistors). Pseudogap is formed near the valence band of the glass due to diffusion of dopant atoms into the glass in calcination. Nanocrystals are generated in the glass in melting process and undergo structure transitions at high temperatures. This approach lets to explain the temperature dependence of conductivity of doped silicate glass from liquid helium up to 1100 K.

**DOI:** 10.1134/S106378422102002X

## INTRODUCTION

Silicate glass doped by transition metal oxides (DSG), well known as a thick-film (or chip) resistor [1], is widely used in electronics and in sensors of physical and chemical factors as a functional material. Therefore, the mechanism of electrical conductivity of DSG and the effect of various factors on it are being investigated in many laboratories [2–4].

DSG is obtained by sintering a mixture of glass powders (particle size 0.1–0.2 μm) and dopant (particle size 0.2–0.5 μm), most often $RuO_2$, ruthenates of bismuth or lead. Typical sintering temperature $T_f$ = 1123 K, duration $\tau_f$ = 600 s for obtaining thick-film resistors, but the conditions may vary depending on the requirements for DSG and its composition. Electron microscopy (Fig. 1) and X-ray diffraction patterns (Fig. 2) show that DSG is a strongly inhomogeneous medium consisting of a glass matrix with crystalline remnants of dopant particles fixed in it. The oxides or oxide compounds used in DSG have high electrical conductivity ($\rho_d = 4 \times 10^{-7}$–$10^{-6}$ Ω m) compared to the original glass ($\rho_g \geq 10^{14}$ Ω m). Therefore, they were taken as centers of localization of charge carriers, and it was believed that carriers pass from one particle to another by variable-range hopping (Mott's mechanism) or by quantum mechanical tunneling through a thin glass layer. Another option was the theory of percolation along electrically conducting chains of contacting dopant particles.

DSG is a unique material [5–16], having electronic conductive in which, when the temperature changes from helium to 1200 K, several modes of electrical conductivity are sequentially realized (Fig. 3). In the literature known to us [1–4] (as well as in others cited there) only sections I and II have been experimentally and theoretically investigated. The interest in section II is due to the conditions of use in electronic equipment, to section I, the search for confirmation of conduction mechanisms based on the tunneling of electrons between dopant particles or on the variable-range hopping between them. Another option was the theory of percolation of contacting dopant particles along electrically conductive chains, despite the fact that estimates led to an average distance of 0.5–2.5 μm between them (Fig. 4):

$$L = d\sqrt[3]{\frac{\pi}{6C}} = d\sqrt[3]{\frac{\pi}{6}\left[1 + \frac{\gamma_d}{\gamma_g}\left(\frac{1}{C_m} - 1\right)\right]}, \qquad (1)$$

where $d$ is the average diameter of the dopant particles, $\gamma_d$ and $\gamma_g$ are the density of the dopant and the glass, respectively. Such distances exclude direct contacts of these particles or tunneling (hopping) of electrons between them.

However, the problem of the origin of the minimum in Fig. 3 remained open in all of these models. It was also found that the percolation threshold on the dependence of the DSG conductivity on the doping level (volume $C$ or mass $C_m$ fraction of the dopant) is significantly lower (1–5 vol %) than follows from the theory ($C_{cr}$ = 16 vol %), or disappears altogether, depending on the DSG composition and sintering conditions [18]. The critical index $t$ of the theory of

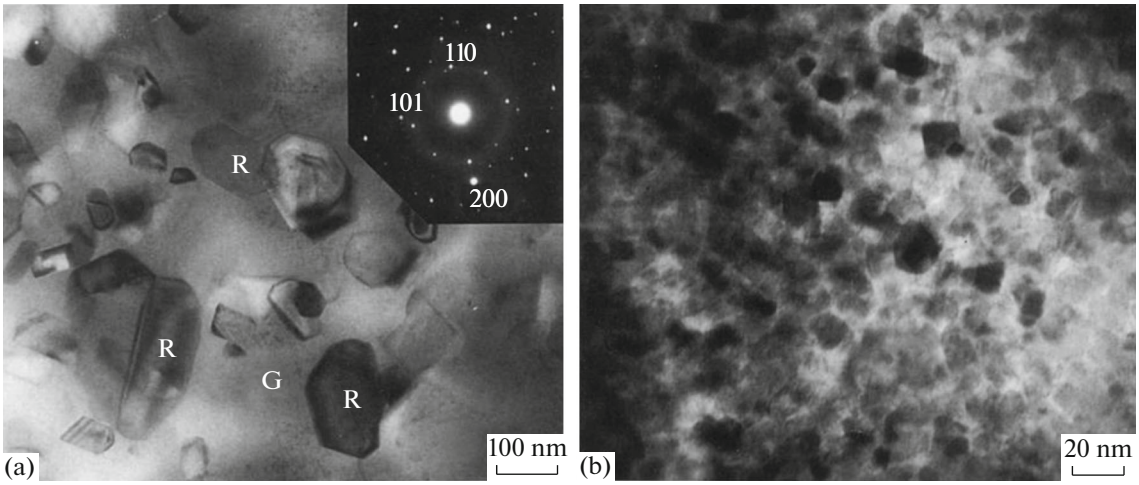


**Fig. 1.** Structure of DSG at nanoscale: (a) from Heraeus 8241. R—$RuO_2$ grains, G—glass. The inset shows electron diffraction from a selected $RuO_2$ grain; (b) from DuPont 8041 paste. Transmission electron micrograph from [17].

leakage $\rho(C) = A(C-C_{cr})t$ in the DSG also significantly differs from the theoretical value ($t = 2.5–5$ versus 1.7).

As Abdurakhmanov et al. [19, 20] showed, the reason for such a discrepancy between experiment and theory was that the researchers did not take into account the possible interaction of the dopant particles and glass during sintering and effect of this interaction on the electrical conductivity of the DSG. This point of view takes place despite the fact (Adachi et al. [21]), that up to 7 at % ruthenium dioxide can be solved in the glass and the diffusion length exceeding 1 μm. Morten et al. [22] found that there is an exchange reaction between the dopant and glass in DSG during sintering, with a partial transition of lead pyrochlores to ruthenium pyrochlores, as a result of which the electrical conductivity of DSG decreases. But the results [21, 22] were not developed further.

The diffusion of dopant atoms into glass during sintering as the cause of the observed decrease or absence of the percolation threshold, the dependence of the DSG conductivity on $T_f$ and $\tau_f$ was substantiated in [20]. It turned out that under typical sintering conditions the diffusion length of the dopant atoms ($l_d \geq 30$ μm for the composition shown in Fig. 2) exceeds the average distance between the dopant particles, i.e., diffusion zones around the dopant particles overlap strongly, transforming the glass into a solid electrically conductive material. The development of this approach made it possible to explain the effect of the size of the dopant particles on the DSG conductivity [20]. The assumption about the existence of silicate nanocrystals of 1–2 nm size in glass and the possibility of structural transitions in them together with the formation of an impurity band due to diffusion of dopant atoms was used in [23] to explain the sharp increase in the DSG resistance (region III in Fig. 3), first discovered by one of the authors of this work [24].

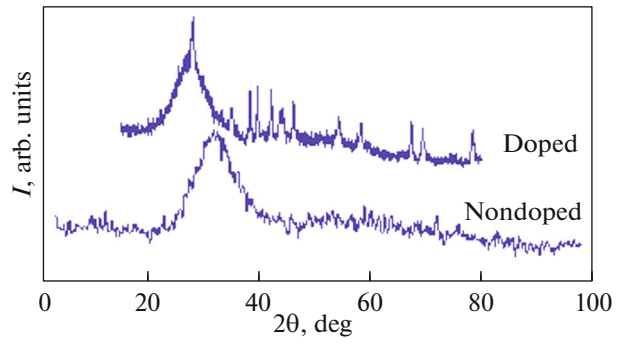


**Fig. 2.** X-ray diffraction patterns of $33SiO_2 + 63PbO + 4Al_2O_3$ glass (charge, by weight) before and after doping (10 wt% $RuO_2$). The crystal reflections in the pattern for doped glass belong to $RuO_2$ [18].

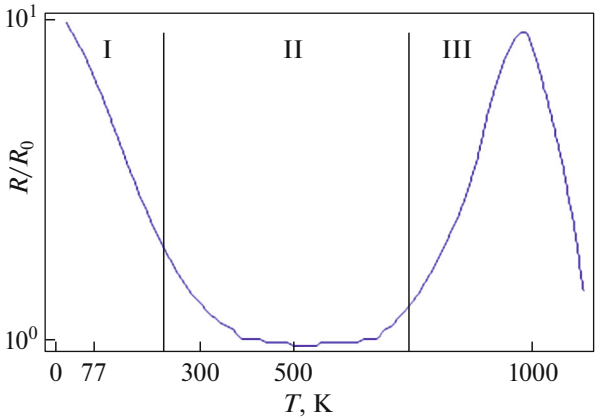


**Fig. 3.** Temperature dependence of DSG resistance (schematically).

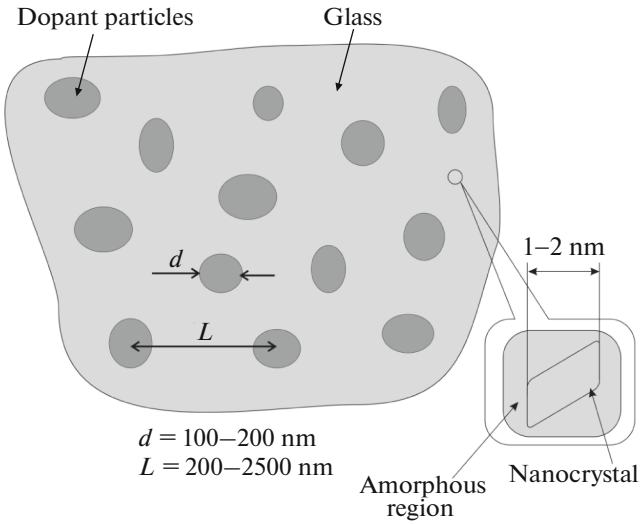


**Fig. 4.** Structure of DSG at micro- and nanoscale.

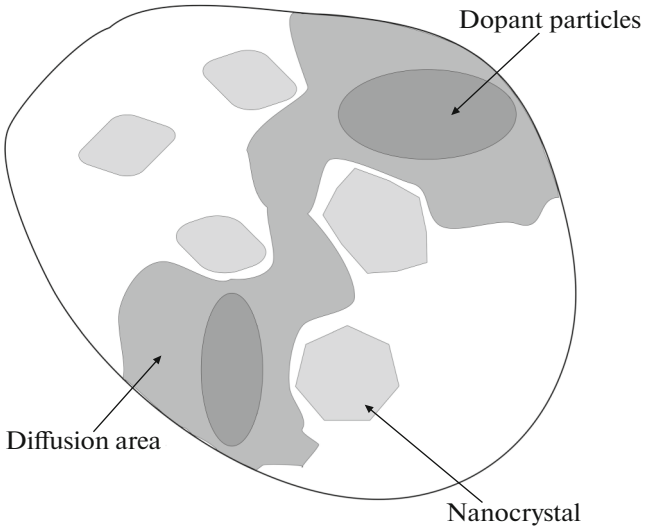


**Fig. 5.** Diffusion zones in the DSG.

The combination of nanocrystals and an impurity band with an electron-phonon coupling (affecting the position of the impurity band [25–29]) explained the minimum $\rho(T)$ and the subsequent "metallic" conductivity $\rho \propto T^{\alpha}$, $\alpha = 1–2$ [5]. It was found [5, 18] that the latter is a consequence of the fusion of the impurity band with the valence band of glass, when the main reason for the temperature dependence of the DSG conductivity is scattering of carriers by ions, phonons, and one another.

But in papers [19, 20], where the diffusion of dopant atoms into glass were considered, it was assumed that the process is isotropic, and glass is homogeneous (the possible effect of nanocrystals on the diffusion of dopant atoms was not taken into account). In reality, the strong inhomogeneity of the DSG (Figs. 1, 2) can lead to the fact that in it the classical laws of diffusion can undergo significant changes [30], and the absence of long-range order creates extended "tails" of the density of states of electrons [31] in the impurity band and at the edge of the valence band of glass. The possible overlap of these "tails" creates a pseudo-gap in the distribution of the density of states of electrons.

In this article we tried to describe some features of the electrical conductivity of DSG that do not depend on the specific composition of the latter. We have based here on the analysis of the published results of studying the mechanisms of electrical conductivity of DSG as well as on the existence of nanocrystals and on the concept of the formation of a pseudogap.

## 1. SILICATE NANOCRYSTALS IN GLASS AND DIFFUSION OF DOPANT ATOMS

Nanocrystals of 1–2 nm size (Fig. 2, Scherer's formula) arise spontaneously in the cooling glass and, therefore, are energetically favorable for the system. In other words, nanocrystals are potential wells. The slowness of glass crystallization, as well as the closeness of the composition of nanocrystals and the rest of the glass mass indicate that these wells are shallow. These potential wells act as the centers of localization of charge carriers, and hopping conduction occurs along them, but their depth has not yet been estimated.

On the other hand, nanocrystals have an increased atomic packing density in comparison with the disordered part of the glass, so the diffusion coefficient of the dopant atoms in them during sintering is reduced. Therefore, the concentration of dopant atoms in nanocrystals will be lower than in glass interlayers between them, and in the DSG we have the distribution of the dopant atoms and electrical conductivity, shown in Figs. 5 and 6 (under the assumption that the electrical conductivity of the DSG is proportional to the concentration of the dopant atoms in the glass).

Thus, the presence of nanocrystals in glass complicates not only the DSG structure, but generates an additional inhomogeneity in the distribution of its electrical conductivity as well.

## 2. PSEUDOGAP AND ELECTRICAL CONDUCTIVITY OF THE DSG

Diffusion of dopant atoms into glass during sintering creates an impurity band in the energy gap of glass [23], similar to diffusion doping of semiconductors. Since the sign of thermoEMF in the DSG is positive [6], this impurity band is located near the top of the valence band of the glass (hole conductivity). It also turned out that the sign of the thermoEMF in the DSG is positive even when the dopant has a negative sign of the thermoEMF. However, the parameters of

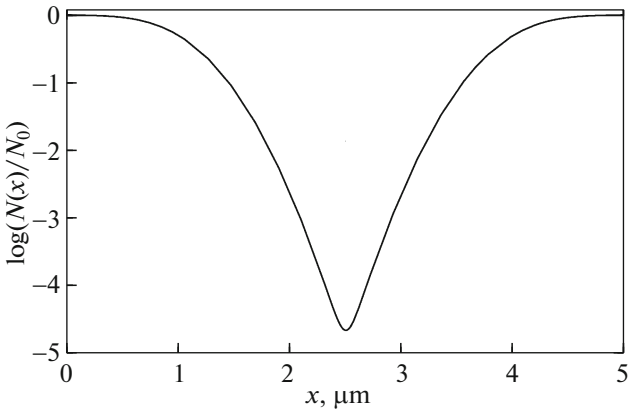


**Fig. 6.** Distribution of dopant atoms between particles. $L$ = 5 μm (see Fig. 4). Modeling by Fick's equation for two diffusion sources [20]. This distribution shows the formation of a pseudogap in the band gap of glass near the ceiling of its valence band.

the impurity band in the DSG were not considered by other authors.

Let us now estimate the parameters of the impurity band in the DSG, based on the known features of the DSG and under certain assumptions.

Such features of the DSG are [6] an extremely low Hall coefficient (the Hall EMF cannot be measured) and the absence of photoconductivity, which indicates a high concentration of free charge carriers (holes), their short free path, and complete ionization of impurity atoms. The upper limit of hole mobility estimated from the noise level is less than $5 \times 10^3$ cm$^2$ V$^{-1}$ s$^{-1}$ for samples of $\rho = 200$ Ω cm, and increases to $3 \times 10^2$ cm$^2$ V$^{-1}$ s$^{-1}$ for samples of $\rho = 0.2$ Ω cm. The hole concentration $p$ for these samples is estimated as $p > 8.3 \times 10^{18}$ cm$^{-3}$ and $p > 1.4 \times 10^{21}$ cm$^{-3}$, respectively.

From these data, under the assumption that the mean free path of carriers is not less than a few angstroms, we estimated the effective mass $m^*$ of holes: $m^* \geq 330\ m_0$ ($m_0$ is the mass of a free electron), i.e. DSG is a heavy fermion system.

It was said above that in low-resistance DSGs near room temperature, after the minimum of $\rho(T)$, "metallic" conductivity sets in due to the merging of the impurity band with the valence band of glass. The temperature coefficient of the band width is $(2–5) \times 10^{-4}$ eV/K [25–29]. Therefore, the gap between the impurity band and the top of the valence band has a width of 60–150 meV at $T = 0$ K.

The width of the impurity band itself can be estimated from the effective mass of holes [32]

$$m^* = \hbar^2/(Ja_0^2), \qquad (2)$$

where $\hbar$ is Planck's constant, $a_0$ is the lattice constant (in the case of oxide glasses, it can be taken approximately equal to the average distance between cations). Estimation of the width of the impurity zone by (2) with $m^* = 3.3 \times 10^2 m_0$, defined above, gives $J = 23$ meV.

It should be noted that DSG, even in a thick-film version (film thickness of about 25 μm), is a bulk material, since the characteristic lengths (of diffusion or free path of electrons), estimated from the upper limit of mobility ($5 \times 10^{-3}$ cm$^2$/V s [6]) are less than 0.1 μm.

The density of states $N_A$ in the impurity band is also related to the effective mass of carriers:

$$N_A = 2J^{-1}\left[\frac{2\pi m^* kT}{h^2}\right]^{3/2} \approx 1.2\times10^{22}\ \text{eV}^{-1}\text{cm}^{-3}. \qquad (3)$$

However, the gap between the impurity band and the valence band of the glass is not empty (pseudogap), since the density of states in the impurity band has a Gaussian distribution and is subject to thermal smearing (of the order of $kT$). A number of mechanisms for the formation of a pseudogap in disordered media have been proposed [31]. In the case of DSG, it makes sense to talk about the minimum density of states $N_m$ in the pseudogap and its change with temperature (Fig. 7) taking into account: a) thermal smearing of the edge $E_V$ of the valence band of the glass and the $E_A$ of the impurity band; b) the shift of the edge $E_A$ of the impurity band towards the valence band of the glass due to the electron-phonon coupling. For convenience of display, the density of states in the valence and impurity bands are taken to be approximately the same; in reality, they differ by about two orders of magnitude.

As seen from Fig. 7, under the above conditions, the minimum density of states $N_m$ in the gap between the impurity and valence bands becomes noticeable even at temperatures above 50 K, and at 300 K it is comparable to the density of states $N_A$ in the impurity band itself. In other words, already at $T \geq 50$ K, the valence band of the glass and the impurity band begin to merge (rudiments of "metallic" conductivity). This trend intensifies with temperature increasing.

Accordingly, the electrical conductivity of the DSG at low temperatures is the sum of the thermoactivation conductivity in the impurity band and the hopping conductivity in nanocrystals:

$$\sigma(T) = \sigma_a + \sigma_h = \sigma_0 T^{0.5}\exp\left[-\frac{1}{kT}\left(E_{G0} - \xi\langle\hbar\omega\rangle \times\left(\coth\frac{\langle\hbar\omega\rangle}{2kT} - 1\right)\right)\right] + \sigma_1 T^{0.5}\exp[-(T_0/T)^{0.25}]. \qquad (4)$$

The first exponential here describes the shift of the impurity band due to the electron – phonon coupling [29], and the second describes the variable-range hopping [31].

An increase in temperature to 700 K leads to begin structural transitions in nanocrystals of silicates formed in glass upon cooling after cooking and after

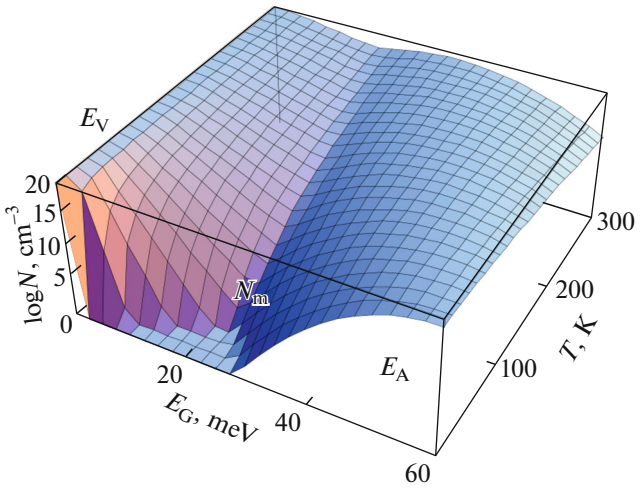


**Fig. 7.** Evolution of the pseudogap $E_G$ and the minimum density of states $N_m$ in it with increasing temperature. $E_V$ and $E_A$—valence and impurity bands, respectively

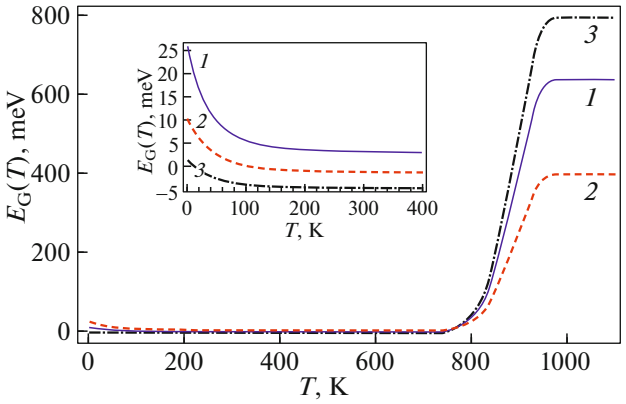


**Fig. 8.** Dynamics of the pseudogap width $E_G(T) = E_V - E_I$. (*1*, *2*, *3*) the glass of different compositions. In the inset, the low-temperature part is shown on an enlarged scale [5, 18].

sintering (see, for example, [33]). These transitions are stretched in temperature due to the spread of atomic bonds in the disordered interlayer around these nanocrystals, in contrast to bulk crystalline samples. Since high-temperature modifications of silicates have a larger interatomic distance, the overlap of the wave functions of impurity atoms decreases and, accordingly, the electrical conductivity of the DSG decreases (section III in Fig. 3). In this case, the thermal smearing of the edge of the valence band and of the impurity band itself increases, but it is not significant due to the fact that the distance between them is 10–20 times greater than the initial width of the gap. This means that the minimum density of states in the gap is already negligible. The behavior of the pseudogap in this region is shown in Fig. 8 for the same conditions as for Fig. 7. As our experiments have shown, after the completion of structural transitions (after the maximum in Fig. 3, $T > 1000$ K), the gap between the valence and impurity bands increases to 0.5–1.5 eV (the $2SiO_2$ PbO glass itself has a width band gap 3.3 eV [34]), and the DSG exhibits activation conductivity with the indicated activation energy (semiconductor).

## CONCLUSIONS

In the DSG, in the entire temperature range studied, two mechanisms of electrical conductivity act simultaneously: hopping over nanocrystals and activation over the impurity band formed by diffusion of dopant atoms into glass. At $T = 0$ K, the gap between the impurity band and the valence band of the glass contains no accessible states for holes. The location of the impurity band is affected by the electron–phonon coupling, so this one comes closer to the top of the glass valence band as temperature increases, so their "tails" begin to overlap, and the conductivity of the DSG increases. At a certain temperature (usually near room temperature), these bands merge, creating a "metallic" conductivity (the carrier concentration stops changing, hopping is ineffective).

As the temperature rises to 700 K, structural transformations begin in silicate nanocrystals, the DSG volume increases, and the overlap of the wave functions of impurity atoms decreases. That splits off the impurity band from the glass valence band and decreases the DSG electrical conductivity. After the completion of structural transitions ($T \geq 1000$ K), the impurity band is fixed in a new position (at a distance of 0.5–1.5 eV from the top of the valence band), and the DSG transforms into a semiconductor with the indicated energy of conductivity activation. Now, the temperature smearing of the band edges and carrier hopping over nanocrystals do not have a noticeable effect on the DSG conductivity.

## FUNDING

The work was carried out within the framework of joint Belarusian–Uzbek scientific and technical grants: MRB-OT-2019-28 of the Ministry of Innovative Development of Uzbekistan and F19UZBG-013 of the Ministry of Education of the Republic of Belarus.

## CONFLICT OF INTEREST

The authors declare that they have no conflicts of interest.

## REFERENCES

1. *Printed Films*, Ed. by M. Prudenziati and J. Hormadaly (Woodhead, Cambridge, 2012).
2. K. S. R. C. Murthy, Int. J. Adv. Res. **7** (4), 238 (2019). https://doi.org/10.21474/IJAR01/8811

3. S. Bindu and M. S. Suresh, Br. J. Appl. Sci. Technol. **6** (4), 342 (2015). https://doi.org/10.9734/BJAST/2015/13337
4. Ming Wen, Sens. Actuators, A **301**, 111779 (2020). https://doi.org/10.1016/j.sna.2019.111779
5. G. Abdurakhmanov, World J. Condens. Matter Phys. **4** (3), 166 (2014). https://doi.org/10.4236/wjcmp.2014.43021
6. G. E. Pike and C. H. Seager, J. Appl. Phys. **48** (12), 5152 (1977).
7. D. P. H. Smith and J. C. Anderson, Thin Solid Films **71**, 79 (1980).
8. K. Flachbart, V. Pavlík, N. Tomašovičová, C. J. Adkins, M. Somora, J. Leib, and G. Eska, Phys. Status Solidi B **205** (1), 399 (1998).
9. W. Schoepe, Physica B **165–166**, 299 (1990).
10. F. Johnson, G. M. Crosbie, and W. T. Donlon, J. Mater. Sci.: Mater. Electron. **8** (1), 29 (1997).
11. J. M. Himelick, PhD Thesis (Purdue Univ., Purdue, 1980). https://docs.lib.purdue.edu/dissertations/AAI8027287/
12. Y. Zheng, J. Atkinson, and R. Sion, J. Phys. D: Appl. Phys. **36**, 1153 (2003). https://doi.org/10.1088/0022-3727/36/9/314
13. C. Grimaldi, in *Printed Films*, Ed. by M. Prudenziati and J. Hormadaly (Woodhead, Cambridge, 2012), Chap. 5.
14. M. Moroz, *IMAPS SoCal'15 Technical Symp.* (Santa Ana, CA, USA, May 12, 2015). http://publication-slist.org/data/M45897/ref-21/Thick Film Systems for Challenging Applications
15. Kenji Adachi and Hiroko Kuno, J. Am. Ceram. Soc. **83** (10), 2441 (2000). https://doi.org/10.1111/j.1151-2916.2000.tb01574.x
16. D. W. Hammer and J. V. Biggers, *Thick Film Hybrid Microcircuit Technology* (Wiley–Interscience, New York, 1972).
17. M. Hrovat, G. Dražič, J. Holc, and D. Belavič, J. Mater. Sci. Lett. **14** (15), 1048 (1995).
18. G. Abdurakhmanov, Doctoral Dissertation in Mathematics and Physics (Inst. Nucl. Phys., Tashkent, 2014).
19. G. Abdurakhmanov and G. S. Vakhidova, Zh. Tech. Phys. **65** (7), 187 (1995).
20. G. Abdurakhmanov, World J. Condens. Matter. Phys. **1** (2), 19 (2011). https://doi.org/10.4236/wjcmp.2011.12004
21. K. Adachi, S. Iida, and K. Hayashi, J. Mater. Res. **9**, 1866 (1994).
22. B. Morten, M. Prudenziati, M. Sacchi, and F. Sirotti, J. Appl. Phys. **83**, 2267 (1988).
23. G. Abdurakhmanov, Am. J. Mater. Sci. **1** (1), 12 (2011). https://doi.org/10.5923/j.materials.20110101.03
24. G. Abdurakhmanov and N. G. Abdurakhmanova, Phys. Status Solidi A **202**, 1799 (2005).
25. H. Y. Fan, Phys. Rev. **78**, 808 (1950).
26. H. Y. Fan, Phys. Rev. **82**, 900 (1951).
27. R. Pässle, Solid-State Electron. **39**, 1311 (1996).
28. H. D. Vasileff, Phys. Rev. **105**, 441 (1957).
29. K. P. O'Donnell and X. Chen, Appl. Phys. Lett. **58**, 2924 (1991).
30. L. A. Bol'shov, P. S. Kondratenko, and L. V. Matveev, Phys.-Usp. **62**, 649 (2019). https://doi.org/10.3367/UFNe.2018.08.038423
31. N. F. Mott and E. A. Davis, *Electron Processes in Non-Crystalline Materials* (Clarendon, Oxford, 1979).
32. A. Feltz, *Amorphe und Glasartige Anorganische Festkörper* (Akademie, Berlin, 1983).
33. F. Liebau, *Structural Chemistry of Silicates* (Springer, Berlin, 1985).
34. T. A. Sidorov, Zh. Prikl. Spektrosk. **6** (1), 98 (1967).